



UDC 636.4:636.083.3

EXPERIMENTAL STUDIES OF THE VENTILATION SYSTEM FOR THE INTAKE OF CONTAMINATED AIR

Vitalii Yaropud

Vinnitsia National Agrarian University, Vinnitsia, Ukraine

Abstract. The article presents the results of experimental research on the determination of the coefficient of reduction of the air flow rate, pressure losses and the necessary power consumption of the exhaust fan, depending on the rotation angle of the damper. The diagram and general view of the laboratory equipment for researching the operation modes of the intake damper, which is the part of the automatic ventilation system for the intake of contaminated air from livestock premises, is given. Its main element is an intake valve with servo drives. The damper is round-shaped and rotates around an axel that lies on its plane.

Based on the results of the first stage of experimental studies of the ventilation system for the intake of polluted air, the dependences of the output air flow rate V_{out} , air consumption q_{out} , the air flow rate reduction coefficient ι , the conditional area of the opening σ_{out} and the fan power consumption N_{damp} on the input speed V_{in} , the angle of rotation of the damper β and the diameter were determined duct D_p . When the dampers are gradually opened by a given angle $\beta(t)$, the inlet velocity $V_{in(t)}$ increases from 11.42 m/s to 17.98 m/s, which is explained by the fact that the damper creates a certain pneumatic resistance and the air flow returns to in the opposite direction, while reducing the overall speed of the incoming air. At the outlet, the airflow velocity $V_{out(t)}$ increases from 0.08 m/s to 17.83 m/s. Moments of opening of the damper occur within 1 s, and a significant increase in speed is observed, both at the inlet and at the outlet, due to the occurrence of turbulent motion. After opening the damper to a given angle, the speed decreases and stabilizes.

According to the results of the second stage of experimental studies of the ventilation system for the intake of contaminated air, the algorithm for controlling the dampers depending on the ratio of gas concentrations was verified. The dependence of the power consumption of the fan N of the ventilation system for the intake of contaminated air on the length of the air duct between the L_0 modules and the air consumption Q_{in} was determined.

Key words: microclimate, ventilation, system, air, pressure, pneumatic resistance, speed, temperature, damper, dependencies, coefficient, livestock premises.

https://doi.org/10.33108/visnyk_tntu2024.04.100

Received 24.09.2024

1. INTRODUCTION

Based on the analysis of modern pig keeping technologies [1–2] in the world and in Ukraine, it was found that the most promising is the new (western) technology. It is characterized by the fact that all livestock is kept on a partially or fully slotted floor in premises that are specialized for different technological groups and divided into isolated sections.

The analysis of microclimate parameters in pig facilities and their impact on pig health [3–5] showed that deviations from optimal conditions lead to worsening of animal health, a decrease in their number and, as a result, a decrease in the profitability of farms. A literature review [6–7] of studies of the impact of microclimate parameters on the physiological condition of pigs confirmed that humidity, temperature, and air flow rate in the pig housing facility have the greatest impact on them.

An analysis of modern microclimate systems in pig facilities [8–9] has shown that the most popular today is the negative pressure ventilation system. This is due to the fact that such a system is easier to operate and maintain and consumes less energy than forced ventilation systems. However, these systems have problems related to three-dimensional ventilation and air injection to animals.

In order to ensure the removal of air from the pigsty room, an appropriate ventilation system was created (Fig. 1). For substantiation of design and technological parameters of the automation of the ventilation system, it is necessary to perform experimental studies.

The automatic ventilation system for the intake of contaminated air (Fig. 1) is located inside the animal facility under the ceiling [10–11]. It consists of a central air duct 1, to which air intake nozzles 2 are connected. Nozzles 2 are located above each stall where animals are kept. At the inlet of the nozzles, there are intake dampers with servo drives 3 and temperature, humidity and air quality sensors 4. The outlet of the central air duct 1 is connected to the exhaust fan 5. The intake dampers 3 and sensors 4 are connected to the control unit 7 by means of electrical wires 6.

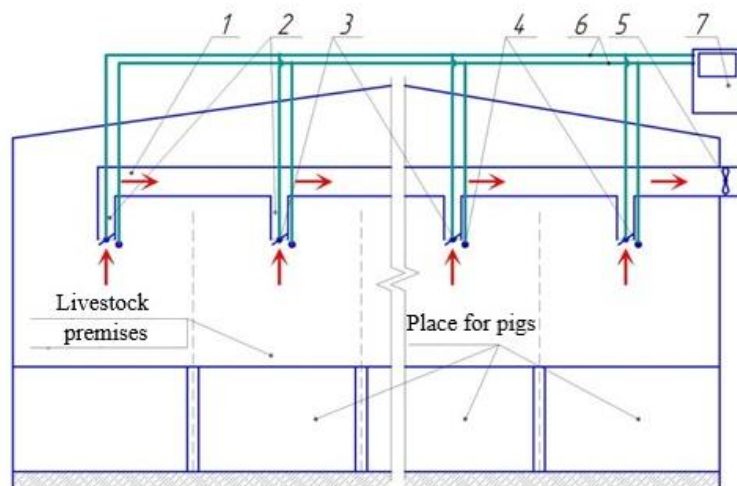


Figure 1. Technological scheme of an automatic ventilation system for the intake of contaminated air:
 1 – central air duct; 2 – nozzles; 3 – intake dampers with servos;
 4 – temperature, humidity and air quality sensors; 5 – exhaust fan;
 6 – electrical wires; 7 – control unit

The automatic ventilation system operates as follows: depending on the air quality above the stalls, which is measured by sensors 4, and the limit values set by the operator, the control unit 7 transmits a signal via electrical wires 6 to the intake dampers 3. If the measured air quality values are below the limit values, the dampers 3 are closed. In other case, the dampers 3 are opened by an angle proportional to the difference between the measured values and the limit values. The exhaust fan 5 draws air through the nozzles 2, forming a stream that moves through the central air duct 1 and out of the room.

Due to the fact that individual group stalls may contain different numbers of animals grouped into different age groups, the concentration of gases (ammonia, carbon dioxide, and hydrogen sulfide) above the stalls may differ [12–14]. Therefore, the automatic ventilation system for the intake of contaminated air should adjust the air flow rate for each machine individually.

2. MATERIALS AND RESEARCH METODS

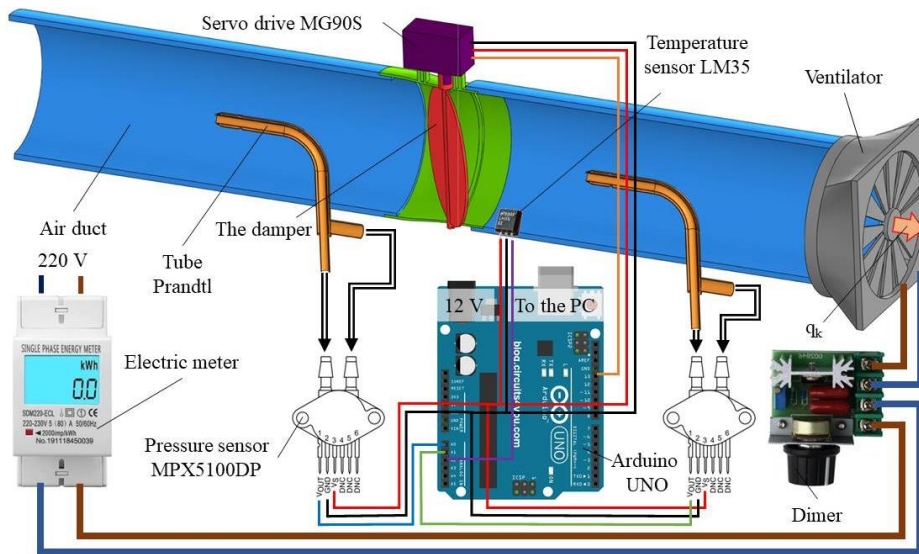
The main element of automatic ventilation systems for the intake of contaminated air is a servo-driven intake damper. The damper has a circular shape and rotates around an axis that lies on its plane. The air flow, moving through the duct in which the damper is located, bends around it, which leads to a certain pneumatic resistance, which reduces the air flow rate and, accordingly, reduces the outlet pressure.

To determine the coefficient of reduction of the air flow rate, pressure losses and the required power consumption of the exhaust fan, depending on the angle of rotation of the damper, laboratory tests will be carried out.

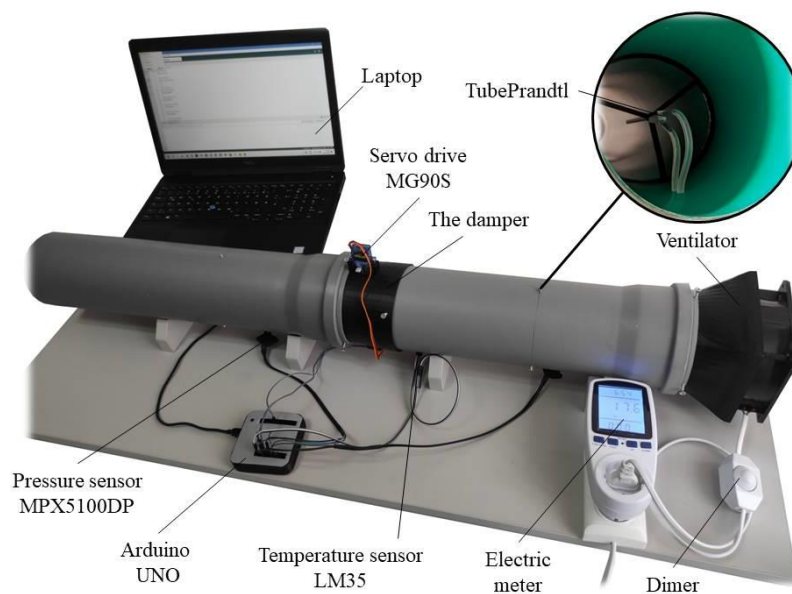
The scheme and general view of the laboratory equipment are shown in Fig. 2. The performance of the exhaust fan was regulated by a dimmer. At the same time, its power consumption was determined using an electric meter. The rotation angle of the damper was set using a servo and an Arduino Uno control board.

The pressure in the duct was determined by an upgraded Prandtl tube that was connected to an MPX5100DP pressure sensor.

The air temperature was determined by an LM35 temperature sensor.



a



b

Figure 2. Schematic (a) and general view (b) of the laboratory equipment for studying the operation modes of the intake valve

The information from the pressure and temperature sensors was read using the Arduino

Uno control board, which is connected to a personal computer with the Arduino IDE software environment installed. The oscilloscope function was used in the Arduino IDE environment to determine the average values and their standard deviation.

Based on the obtained data of total p_1 and static p_2 pressures, the air flow rate was determined and recalculated to the outlet area:

$$V = \sqrt{\frac{2\gamma}{\gamma-1} gRT \left(1 - \left(\frac{p_2}{p_1} \right)^\gamma \right)}, \quad (1)$$

$$q = 3600V \frac{\pi D_p^2}{4} = 900\pi D_p^2 \sqrt{\frac{2\gamma}{\gamma-1} gRT \left(1 - \left(\frac{p_2}{p_1} \right)^\gamma \right)}, \quad (2)$$

where T is the air temperature, K; γ is the air adiabatic coefficient, $\gamma = 1.4$; g is the free fall acceleration, $g = 9.8 \text{ m/s}^2$; R is the universal gas constant, $R = 8.31 \text{ J/(mol}\cdot\text{K)}$; D_p is the duct diameter, m; V is the air flow velocity, m/s; q is the air flow rate, m^3/h .

The research factors are: the damper rotation angle β , the air flow velocity V created by the exhaust fan after the damper at a distance of $3D_p$ (330 mm). The levels and intervals of the factors are shown in Table 1.

Table 1. Levels and intervals of research factors

Level	Damper rotation angle β , °	Air flow rate V , m/s
- 1.00	10	2
- 0.75	20	4
- 0.50	30	6
- 0.25	40	8
0	50	10
+ 0.25	60	12
+ 0.50	70	14
+ 0.75	80	15
+ 1.00	90	18

The research criteria were the air flow rate V in front of and after the damper at a distance of $3D_p$ (330 mm) and the power consumption of the exhaust fan N .

The research was conducted according to a full-factorial plan with a total number of experiments $5^3 = 125$.

The next step is to study the ventilation system for the intake of contaminated air.

The diagram of the laboratory simulator of the ventilation system for polluted air intake is shown in Fig. 3. This simulator consists of 4 identical modules, which are connected by means of an air duct with a length L and a diameter $D = 110 \text{ mm}$. An exhaust fan was connected to one end of the duct, the performance of which was regulated by a dimmer. The dimmer is connected to a 220 V circuit through an electric meter, the function of which is to determine the power consumption of the exhaust fan.

The upper part of the module has an air duct fitting (tee or angle), to the lower part of

which a damper with servos is attached. The damper rotation angle was set using a servo and an Arduino MEGA 2560 control board. An upgraded Prandtl tube based on the MPX5100DP pressure sensor, an LM35 analogue temperature sensor, and an MQ-2 gas sensor are mounted in the fitting. The information from the pressure, temperature, and gas sensors was read using the Arduino MEGA 2560 control board, which is connected to a personal computer with the Arduino IDE software environment installed. In the Arduino IDE environment, the oscilloscope function was used to determine the average values and their standard deviation.

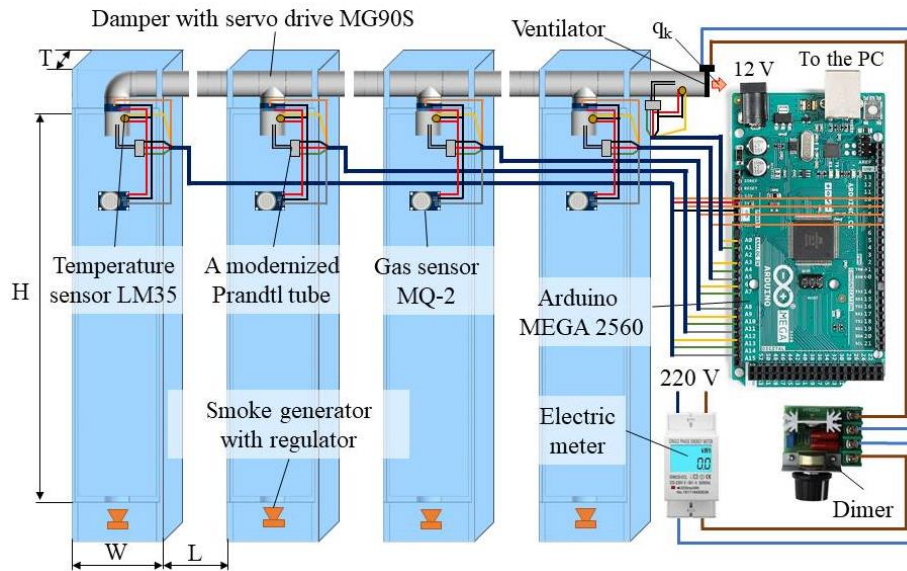


Figure 3. Diagram of the laboratory test stand for the study of ventilation system for polluted air intake

To simulate indoor air pollution, a smoke generator with a smoke flow regulator is installed in the lower part of the module.

The research factors are as follows (Table 2):

- air flow rate Q_{in} , created by the exhaust fan;
- length of the duct between the modules L ;
- the ratio of gas concentration in each module $n_{g1}:n_{g2}:n_{g3}:n_{g4}$.

In Table 2, the gas concentration ratio factor is chosen by randomizing numbers from 1 to 5. The ratio of 1:1:1:1 is the control.

The criteria for the study were the air flow rate V in front of the damper of each module and its deviation from the average and the power consumption of the exhaust fan N .

The research was conducted according to a complete factorial design with a total number of experiments $5^3 = 125$.

Table 2. Levels and intervals of research factors

Levels	Air flow rate Q_{in} , m ³ /h	Length of the duct between the modules L_0 , m	Ratio of gas concentration $n_{g1}:n_{g2}:n_{g3}:n_{g4}$
- 1,00	100	1	1:1:1:1
- 0,50	200	2	2:1:2:1
0	300	3	2:1:2:4
+ 0,50	400	4	4:5:2:1
+ 1,00	500	5	3:4:1:5

3. RESULTS AND DISCUSSION

According to the results of the first stage of experimental studies conducted on the laboratory simulator, the dynamics of speed changes at the inlet and outlet of the damper V_{in} , V_{out} during its rotation by a given angle β was determined (Fig. 4).

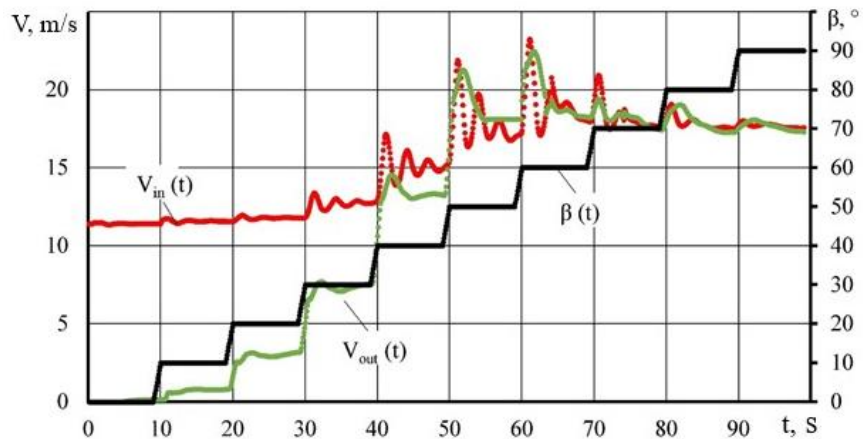


Figure 4. dynamics of speed changes at the inlet and outlet of the damper $V_{in(t)}$, $V_{out(t)}$ during its rotation by a given angle $\beta(t)$

Figure 4 shows that when the dampers are gradually opened by a given angle $\beta(t)$, the inlet velocity $V_{in}(t)$ increases from 11.42 m/s to 17.98 m/s. This can be explained by the fact that the damper creates a certain pneumatic resistance and the air flow turns in the opposite direction, reducing the overall velocity of the incoming air. Also, at the outlet, the air flow velocity $V_{out}(t)$ increases from 0.08 m/s to 17.83 m/s. Interesting are the moments of the damper opening, which occur within 1 s. Here we observe a significant increase in velocity, both at the inlet and outlet. This is due to the appearance of turbulent motion. Then, after opening the damper to a given angle, the velocity decreases and stabilizes. Therefore, in further calculations, we will use the stabilized value of the velocity V_{out} .

By changing the inlet air flow rate with the help of a dimmer, which was controlled by the value of V_{in} ($t = 100$ s) and the rotation angle of the damper β in accordance with Table 1.

Having constructed a three-dimensional graph of the experimental data (Fig. 5), it is possible to approximate them in the Wolfram Cloud software package using the NonlinearModelFit function.

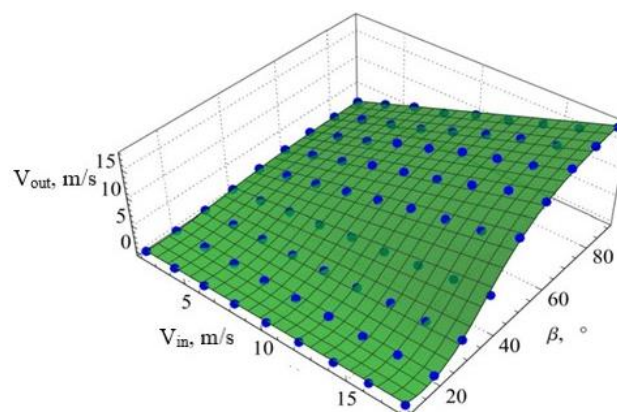


Figure 5. Dependence of the output air flow velocity V_{out} on the inlet velocity V_{in} and the damper rotation angle β

As can be seen from Fig. 5, the experimental data (blue dots) form a linear dependence on the inlet airflow velocity V_{in} and an ‘arctg’ dependence on the damper rotation angle β . Thus, in the coded form, the equation is as follows:

$$V_{out} = 5,42863 + 5,59269 X_1 \times \arctg(1,35715 + 3,31601 X_2 + 1,98998 X_2^2), \tag{3}$$

where X_1, X_2 are the coded values of the V_{in} and β factors, respectively. The results of the static processing of equation (3) are presented in Table 3.

Table 3. Results of static processing of equation (3)

Coefficient ¹	Value	Error	Student's criterion	Probability
a ₁	5.42863	0.443587	12.238	1.19699·10 ⁻¹⁹
a ₂	5.59269	1.45529	3.84301	0.000250417
a ₃	1.35715	1.17623	1.15381	0.252194
a ₄	3.31601	3.79226	0.874414	0.384647
a ₅	1.98998	2.85363	0.69735	0.487712

$$^1V_{out} = a_1 + a_2 x_1 \arctg(a_3 + a_4 x_2 + a_5 x_2^2)$$

Having decoded equation (6.1), we have:

$$V_{out} = 0.044571 + 0.688783 V_{in} \times \arctg(0.331332 - 0.0435501 \beta + 0.00130178 \beta^2). \tag{4}$$

The graphical interpretation of equation (4) is shown in Fig. 5 (green surface).

Taking into account the diameter of the duct D_p , the air flow rate q_{out} through the damper can be calculated by the following dependence:

$$q_{out}(V_{in}, \beta, D_p) = (3600 \pi D^2/4) \cdot (0.044571 + 0.688783 V_{in} \times \arctg(0.331332 - 0.0435501 \beta + 0.00130178 \beta^2)) = 126.022 D_p^2 + 1947.49 D_p^2 V_{in} \times \arctg(0.331332 - 0.0435501 \beta + 0.00130178 \beta^2). \tag{5}$$

The air flow rate reduction rate ι through the damper can be calculated using the following formula:

$$\iota = V_{out}/V_{in} = 0.044571/V_{in} + 0.688783 \times \arctg(0.331332 - 0.0435501 \beta + 0.00130178 \beta^2). \tag{6}$$

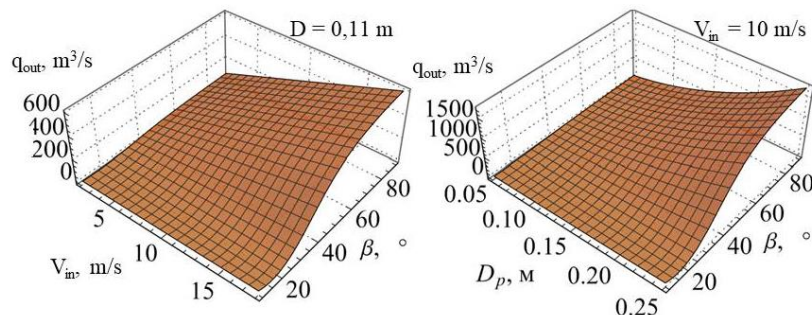


Figure 6. Dependence of the air flow rate q_{out} through the damper on the inlet velocity V_{in} and the rotation angle of the damper β

The graphical interpretation of dependence (6) is presented in Fig. 7.

From Fig. 7 it can be seen that the inlet velocity V_{in} in the specified range does not affect the coefficient of air flow rate reduction ι . That is, the coefficient ι depends only on the angle of rotation of the damper β , which is reasonable.

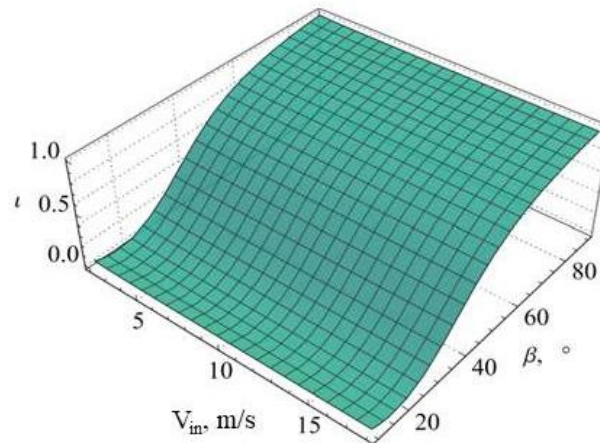


Figure 7. Dependence of the coefficient of air flow rate reduction ι over the damper on the inlet velocity V_{in} and the damper rotation angle β

The dependence of the power N_{damp} consumed by the fan using the Wolfram Cloud software package in coded form can be represented as follows:

$$N_{damp} = 49.7015 + 41.3971 x_1 + 20.1834 x_1^2 - 4.84245 x_2 - 3.34054 x_1 x_2 - 0.324002 x_2^2, \tag{7}$$

where x_1, x_2 are the coded values of the V_{in} and β factors, respectively.

The results of the static processing of equation (7) are shown in Table 4.

Table 4. Results of static processing of equation (7)

Coefficient	Value	Error	Student's criterion	Probability
a_{00}	49.7015	0.439998	112.958	$1.63941 \cdot 10^{-85}$
a_{10}	41.3971	0.359387	115.188	$3.81587 \cdot 10^{-86}$
a_{20}	- 4.84245	0.359387	- 13.4742	$1.01467 \cdot 10^{-21}$
a_{12}	- 3.34054	0.55676	- 5.99996	$6.48143 \cdot 10^{-8}$
a_{11}	20.1834	0.634487	31.8106	$2.7262 \cdot 10^{-45}$
a_{22}	- 0.324002	0.634487	- 0.510652	0.611095

Having decoded equation (7), we have:

$$N_{damp} = 30.3252 - 0.0166696 b - 0.610717 V - 0.0104392 b V + 0.315365 V^2, \tag{8}$$

Graphical interpretation of equation (8) is shown in Fig. 8.

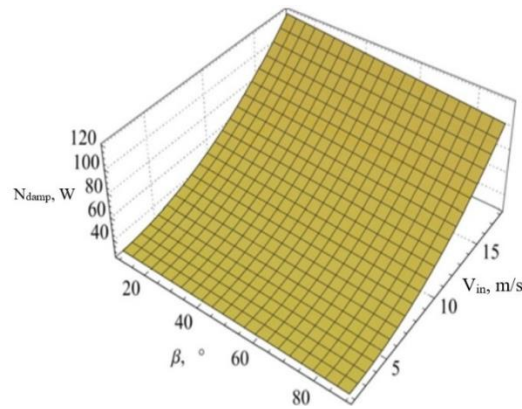


Figure 8. Dependence of the fan power consumption N_{damp} on the input speed V_{in} and the damper rotation angle β

Fig. 8 demonstrates that as the flow rate V_{in} grows, the motor power N_{damp} increases. Also, when the damper is closed, there is an increase in power consumption N_{damp} by 18–20%.

To further justify the algorithm of operation of the control unit of the automatic ventilation system for the intake of contaminated air, we convert dependence (4) to the conditional area of the holes σ_{out} in the air intake nozzles. To do this, we will use the identity that the air flow rates at the intake and outlet of the nozzle are the same. Then:

$$V_{in} \sigma_{in} = V_{out} \sigma_{out}, \tag{9}$$

$$\sigma_{out} = (V_{in}/V_{out}) \sigma_{in}, \tag{10}$$

$$\sigma_{out} = \sigma_{in} V_{in} / (0.044571 + 0.688783 V_{in} \times \arctg(0.331332 - 0.0435501 \beta + 0.00130178 \beta^2)), \tag{11}$$

where σ_{in} is the area of the nozzle.

Since the diameter of the nozzle was 0.11 m, then equation (11) will look as follows

$$\sigma_{out} = 0.00950332 V_{in} / (0.044571 + 0.688783 V_{in} \times \arctg(0.331332 - 0.0435501 \beta + 0.00130178 \beta^2)). \tag{12}$$

The graphical interpretation of dependence (12) is shown in Fig. 9, which clearly shows that the conditional area of the holes σ_{out} in the air intake nozzles depends only on the angle of rotation of the damper β . That is, the obtained dependence can be further used.

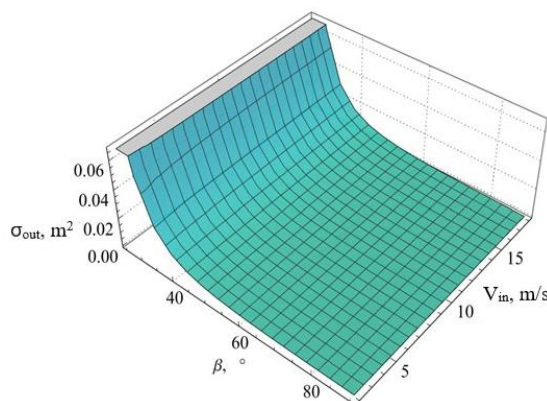


Figure 9. Dependence of the conditional outlet area σ_{out} at the nozzle for air intake on the inlet velocity V_{in} and the damper rotation angle β

Having removed the insignificant expression $0.044571/V_{in}$, we eventually obtain

$$\sigma_{out} = 0.01379726 / \arctg(0.331332 - 0.0435501 \beta + 0.00130178 \beta^2). \quad (13)$$

Dependence (13) can be used as a transfer function of the control system.

4. CONCLUSIONS

1. According to the results of the first stage of experimental studies on the ventilation system for the intake of contaminated air, the dependence of the output air flow rate V_{out} , air flow rate q_{out} , air flow rate reduction factor ι , conditional area of the opening σ_{out} , and fan power consumption N_{damp} on the input speed V_{in} , damper rotation angle β , and duct diameter D_p were determined.

2. Based on the results of the second stage of experimental studies of the ventilation system for the intake of polluted air, the algorithm for controlling the dampers depending on the ratio of gas concentrations was tested. The dependence of the fan power consumption N of the ventilation system for polluted air intake on the length of the duct between the modules L_0 and the air flow rate Q_{in} was determined.

References

1. Lykhach V. Ya., Lykhach A. V. (2020). Technological innovations in pig breeding: monograph. Kyiv: FOP Yamchynskiy O. V., 291 p.
2. Povod M., Bondarska O., Lykhach V., Zhizhka S., Nechmilov V., Dudin V. (2021). Technology of production and processing of pig products: a study guide. Kyiv: Scientific and Methodological Center of VFPO. 360 p.
3. Samokhina E. A., Povod M. G., Mylostyviy R. V. (2018) Microclimate parameters in piggery premises in summer under different ventilation systems and their influence on the productivity of lactating sows and the growth of suckling piglets. Bulletin of the Sumy National Agrarian University. Series: Livestock, issue 2, pp. 218–223.
4. Zhizhka S., Povod M. (2019) Reproductive qualities of sows depending on microclimate systems throughout the year. Bulletin of the Sumy National Agrarian University. Series: Livestock, issue 4 (39), pp. 85–91.
5. Collin A., Vaz M. J., Le Dividich J. (2002) Effects of high temperature on body temperature and hormonal adjustments in piglets. *Reprod. Nutr. Dev.*, 42, pp. 45–53. <https://doi.org/10.1051/rnd:2002005>.
6. Tkachuk O. D. (2010) Influence of microclimate on the main indicators of pig resistance. Bulletin of the Poltava State Agrarian Academy, no. 2, pp. 136–140. Available at: <https://www.pdau.edu.ua/sites/default/files/visnyk/2010/02/136.pdf>.
7. Vranken E. (1999) Analysis and optimisation of ventilation control in livestock buildings. PhD Diss, no. 392. Leuven, Belgium: Catholic University Leuven, Laboratory for Agricultural Buildings Research..
8. Shulga M. O., Aleksakhin O. O., Shushlyakov D. O. (2014). Heating and gas supply and ventilation: training. manual. Hark. national city university farm named after O. M. Beketova. XNUMG, 191 p.
9. Duan Z., Changhong Z., Zhang X., Mustafa M., Alimohammadisagvand B., Hasan A., Zhao X. (2012) Indirect evaporative cooling: Past, present and future potentials. *Renewable and Sustainable Energy Reviews*, vol. 16, pp. 6823–6850. <https://doi.org/10.1016/j.rser.2012.07.007>
10. Kaletnik G. M., Yaropud V. M. Mechatronic system of microclimate provision of livestock premises. Pat. № 148970 UA, IPC A01K 1/00, F24F 3/00, F24F 3/044, F24F 3/14, F24F 6/12, F24F 7/007; № u 202102133; statement 04/22/2021; published 05.10.2021, Bul. № 40. 7 p.
11. Kaletnik G. M., Yaropud V. M. Mechatronic system of microclimate provision of livestock premises. Pat. № 127795 UA, IPC (2023.01) A01K 1/00, F24F 3/00, F24F 3/044 (2006.01), F24F 3/14 (2006.01), F24F 6/12 (2006.01), F24F 7/007 (2006.01), F24F 11/00; № a 2021 02134; statement 04/22/2021; published 03.01.2024, Bul. № 1.
12. Kaletnik G. M., Yaropud V. M. (2023) Experimental studies of the effectiveness of systems for providing a negative pressure microclimate in livestock premises. Design, production and operation of agricultural machines, issue 53, pp. 66–84. <https://doi.org/10.32515/2414-3820.2023.53.66-84>
13. Aliev E. B., Gavrilchenko O. S., Klyus A. V. Justification of the composition of energy-saving technical means to ensure the microclimate in livestock premises. Modern problems and technologies of the agricultural sector of Ukraine: Collection. scientific theses (November 21, 2019) / For science. Ed. V. S. Lukacha [and others]. Nizhin. P. 8–16.

14. Aliev E. B., Yaropud V. M., Bilous I. M. (2020) Justification of the composition of the energy-saving system for microclimate provision in piggery premises. *Vibrations in engineering and technology*, no. 2 (97), pp. 29–137. <https://doi.org/10.37128/2306-8744-2020-2-14>

УДК 636.4:636.083.3

ЕКСПЕРИМЕНТАЛЬНІ ДОСЛІДЖЕННЯ ВЕНТИЛЯЦІЙНОЇ СИСТЕМИ ЗАБОРУ ЗАБРУДНЕНОГО ПОВІТРЯ

Віталій Яропуд

Вінницький національний аграрний університет, Вінниця, Україна

Резюме. Представлено результати експериментальних досліджень визначення коефіцієнта зниження швидкості потоку повітря, втрат тиску й необхідної споживаної потужності витяжного вентилятора, від кута повороту заслінки. Наведено схему і загальний вигляд лабораторного обладнання для дослідження режимів роботи забірної заслінки, що входить до складу автоматичної вентиляційної системи забору забрудненого повітря з тваринницьких приміщень. Основним елементом її є забірні заслінки з сервоприводами. Заслінка має круглу форму й обертається навколо осі, яка лежить на її площині.

За результатами першого етапу експериментальних досліджень вентиляційної системи забору забрудненого повітря визначено залежності вихідної швидкості потоку повітря V_{out} , витрат повітря Q_{out} , коефіцієнта зниження швидкості потоку повітря λ , умовної площі отвору σ_{ot} і споживаної потужності вентилятора N_{damp} від вхідної швидкості V_{in} , кута повороту заслінки β і діаметра повітропроводу D_p . При поетапному відкритті заслінок на заданий кут $\beta(t)$, швидкість на вході $V_{in}(t)$ збільшується з 11,42 м/с до 17,98 м/с, що пояснюється тим, що заслінка створює певний пневматичний опір і потік повітря повертається в протилежному напрямку, зменшуючи при цьому загальну швидкість вхідного повітря. На виході швидкість потоку повітря $V_{out}(t)$ збільшується з 0,08 м/с до 17,83 м/с. Моменти відкриття заслінки відбуваються впродовж 1 с, і спостерігається значне підвищення швидкості як на вході, так і на виході, у зв'язку із виникненням турбулентного руху. Після відкриття заслінки на заданий кут швидкість спадає і стабілізується.

За результатами другого етапу експериментальних досліджень вентиляційної системи забору забрудненого повітря перевірено алгоритм роботи керування заслінками залежно від співвідношення концентрацій газів. Визначено залежність споживаної потужності вентилятора N вентиляційної системи забору забрудненого повітря від довжини повітропроводу між модулями L_0 і витрат повітря Q_{in} .

Ключові слова: мікроклімат, вентиляція, система, повітря, тиск, пневматичний опір, швидкість, температура, заслінка, залежності, коефіцієнт, тваринницьке приміщення.

https://doi.org/10.33108/visnyk_tntu2024.04.100

Отримано 24.09.2024